Natural Resources for Human Health
eISSN: 2583-1194

Original Research

Received 11 July 2026
Revised 12 Aug 2026
Accepted 26 Aug 2026

Natural Resources for Human Health 2026, Vol. 6 (19s): 837–847

KEYWORDS:
Metabolic syndrome, Polyherbal nanosuspension, Tinosporacordifoliaand, Momordica charantia, Enzyme modulation.

Development and in Vivo Evaluation of an Optimized Polyherbal Nanosuspension for the Management of High-Fat Diet-Induced Metabolic Syndrome in Wistar Rats.

Ravindra A. Patil[1]*, AHM Viswanathswamy[2], Popat S. Kumbhar[3]

[1]Tatyasaheb Kore College of Pharmacy, Warananagar.
[2]KLEU College of Pharmacy Hubali
[3]Tatyasaheb Kore College of Pharmacy, Warana University, Warananagar., Maharashtra, 416113, India
Email: rapatil.tkcp@gmail.com

ABSTRACT: High-fat diet (HFD)–induced rat models closely mimic the multifactorial pathophysiology of human metabolic syndrome (MS). In this study, a polyherbal formulation (PHF) was developed from alcoholic extracts of Tinospora cordifolia, Momordica charantia, Trigonella foenum-graecum, Acorus calamus, and Tecomella undulata and evaluated for in vivo therapeutic efficacy in HFD-induced Wistar rats. Three formulations of nanosuspension (PHF-A, PHF-B, and PHF-C) were prepared with varying concentrations of HPMC and Tween 80. Among these, PHF-A (HPMC 0.6%, Tween 80 0.3%) demonstrated optimal stability and performance, with particle size of 117 nm, zeta potential of −0.30 mV, PDI of 0.372, pH 6.0, viscosity 93.87 cP, and excellent redispersibility over 90 days. Acute oral toxicity assessment (2000 mg/kg) confirmed the safety of PHF-A. In HFD-induced Wistar rats, PHF-A (400 mg/kg) produced significant improvements in metabolic parameters, including reductions in body weight, triglycerides, total cholesterol, LDL, SGPT, and SGOT, along with increases in HDL and decreases in antioxidant enzyme levels of SOD, GSH, and CAT. Collectively, these findings demonstrate that the optimized PHF exerts multi-target therapeutic effects against HFD-induced MS, supporting its potential as a candidate formulation for the management of metabolic syndrome.

1. INTRODUCTION

Metabolic syndrome (MS) comprises a cluster of metabolic disturbances—including insulin resistance, dyslipidemia, hypertension, and central obesity—that collectively increase the risk of type 2 diabetes and cardiovascular disease [1]. However, in the clinical settings, MS is attributed based on the diagnosis of three out of five metabolic parameters. Its rising global prevalence, driven by sedentary lifestyles and calorie-dense diets, highlights the need for therapeutic strategies that can target multiple pathological pathways simultaneously [2]. However, current pharmacological approaches primarily address individual components of MS and are often limited by adverse effects and suboptimal long-term outcomes [3]. These limitations underscore the importance of developing integrated, multi-target interventions capable of modulating the complex pathophysiology of MS. Consequently, there is growing interest in complementary and alternative medicine, particularly polyherbal formulations, which offer a multi-target approach through the synergistic actions of diverse bioactive constituents, making them well-suited for managing the complex pathology of MS [4]. The therapeutic potential of medicinal plants in MS is largely attributed to their diverse phytochemical constituents, including alkaloids, flavonoids, and saponins, which

modulate metabolic pathways through antioxidant, anti-inflammatory, and insulin-sensitizing mechanisms [5]. The selected plants—*Tinospora cordifolia, Momordica charantia, Trigonella foenum-graecum, Acorus calamus, and Tecomella undulata*—have individually demonstrated antidiabetic, lipid-lowering, and antioxidant activities [6]. However, their integration into a singleand systematic evaluation in a MS model remain largely unexplored [7]. In this context, the present study was designed to develop and optimize a PHN, characterize its physicochemical stability, and evaluate its therapeutic efficacy in an HFD-induced MS rat model**,** with a particular focus on metabolic and hepatoprotective outcomes. This approach provides a rational, evidence-based framework for translating traditional herbal combinations into reproducible and experimentally validated therapeutic formulations.

MATERIAL AND METHODS

Plant Materials and Reagents

Alcoholic extracts of *Tinospora cordifolia* (TC), *Momordica charantia* (MC), *Trigonella foenum-graecum* (TG), *Acorus calamus* (AC), and *Tecomella undulata* (TU) were procured from the Sahydri Hill region, Kolhapur, local farms and from crude drug suppliers. Plant materials were shade-dried and ground to a coarse powder. All chemicals and solvents were of analytical grade (E. Merck, SD Fine, CDH Chemicals). Tween 80 and HPMC were sourced from Sigma-Aldrich; methyl paraben from Merck Life Science; lemon oil from HiMedia Laboratories.

Formulation of Polyherbal Nanosuspension

A 100 ml PHN (1:1:1:1:1) was made by triturating equal volumes of each extract. Weighed dry extracts were transferred to a clean mortar, Tween 80 and HPMC were added, and the mixture was triturated by progressively adding cleaned water to guarantee uniform dispersion. The mixture was then transferred to glass beaker and stirred at 1200 rpm, 10 min, later it was sonicated at short pulses. The preservative methyl paraben and the flavouring lemon oil were added by continuous trituration [8]. Three trial batches differing in HPMC and Tween 80 concentrations were prepared.

Table 1: Formulation ccomposition of polyherbal nanosuspension batches

Sr. No.	Ingredient	PHN-A	PHN-B	PHN-C
1	**AC of *T. cordifolia* (g)**	0.5	0.5	0.5
2	**AC of *M. charantia* (g)**	0.5	0.5	0.5
3	**AC of *T. foenum-graecum* (g)**	0.5	0.5	0.5
4	**AC of *A. calamus* (g)**	0.5	0.5	0.5
5	**AC of *T. undulata* (g)**	0.5	0.5	0.5
6	**Tween 80 (% v/v)**	0.3	0.2	0.1
7	**HPMC (%)**	0.6	0.4	0.2
8	**Methyl paraben (% v/v)**	0.2	0.2	0.2
9	**Lemon oil (% v/v)**	0.01	0.01	0.01
10	**Distilled purified water (mL)**	Up to 100	Up to 100	Up to 100

Physicochemical Evaluation of PHN

Sedimentation Volume

10 mL of PHN was transferred to a graduated cylinder and left undisturbed at room temperature (RT). After 24 h, the original volume (V_0) and sediment volume (Vu) were measured. Sedimentation volume was calculated using the formula: F=Vu/Vo.

Redispersibility and Flow Rate

Redispersibility was calculated as the number of inversions required for complete redispersion after sedimentation. The flow rate (mL/s) was measured by timing the passage of 10 mL using a clean graduated pipette (n=3).

pH and Viscosity

The pH was measured at RT using a calibrated digital pH meter (n=3). Viscosity was measured in cP using a Brookfield viscometer running at RT and a constant rotational speed of 100 rpm.

Particle Size, PDI, and Zeta Potential

Particle size, polydispersity index (PDI), and zeta potential were assessed using a HORIBA nanoparticle analyzer (SZ-100) based on Dynamic Light Scattering (DLS) and Electrophoretic Light Scattering (ELS) principles. Samples were diluted in distilled water before the measurement of Zeta potential, PDI, and mean particle size were measured at RT.

Crystal Growth Study

Physical stability in relation to crystal/particle formation was assessed by comparing particle size before and after predetermined storage times at RT. Particle or crystal growth was indicated by any change in particle size.

Accelerated Stability Study (PHN-A)

The optimized batch PHN-A was evaluated over 90 days (0, 30, 60, and 90 days) under accelerated circumstances. Sedimentation volume, particle size, zeta potential, PDI, and viscosity were measured at each interval.

Experimental Animals

Healthy Wistar rats of either sex, aged 6–8 weeks, weighing 150–180 g, were housed in standard conditions (22 ± 2°C, 50–60% RH, 12 h light/dark). Animals have unlimited access to food and water. All procedures were conducted in accordance with IAEC guidelines (Clearance Nos.: TKCP/2025/03/ID; IAEC/BiRD/Sangli/2024–25/07/22).

Experimental Design

Thirty rats were randomly allocated into five groups (n=6):

Diet and Treatment Regimen

The 60% kcal fat, 20% kcal protein, and 20% kcal carbohydrates that comprised the HFD were supplemented with 10% fructose drinking water. All groups were fed a high-fat diet for 16 weeks, with the exception of the Normal control group. Oral PHN and standard drug Orlistat wereadministeredin HFD rats after 12 weeks for duration of 4 weeks. Treatments was given as shown in the following table:

Table 2: Experimental Design and Treatment Regimen

Group	Treatment	Dose / Route
Group I	Normal Control (Standard diet)	Standard diet, Oral.
Group II	HFD Disease Control	High-fat diet only
Group III	HFD + Standard Drug (Orlistat)	45 mg/kg, oral.
Group IV	HFD + PHN Low Dose (LD)	200 mg/kg, oral.
Group V	HFD + PHN High Dose (HD)	400 mg/kg, oral.

Acute Toxicity Study (OECD 423)

PHN was administered at 2000 mg/kg by oral gavage to sixrats. Animals were observed at 30 min, 4 h, 24 h, 48 h, 7 days, and 14 days for signs of toxicity [9].

Assessments

Body weight, fasting blood glucose, insulin, triglycerides, total cholesterol, HDL, and LDL were measured at day 0, 30, 60, 90, and 120. ALT andASTwere measured at day 90 and 120. OGTT was performed at the end of the study. Adipocyte index and liver weight were recorded at sacrifice.

Natural Resources for Human Health
eISSN: 2583-1194

Histopathological Examination

Hematoxylin and eosin (H&E) was used to stain the liver, Heart and Pancrease tissues after they were sectioned at 5 μm, paraffin-embedded, and fixed in 10% neutral buffered formalin. Hepatocyte, pancreatic, cardiac architecture, fatty vacuolation, sinusoidal congestion, degeneration, tissue damage, inflammatory infiltration were evaluated by a blinded pathologist [11].

Statistical Analysis

The data is expressed as mean ± SEM (n=6) andnormality was confirmed using the Kolmogorov-Smirnov test following a one-way ANOVA, Dunnett's multiple comparison test was used. The threshold for statistical significance was set at $p < 0.05$.

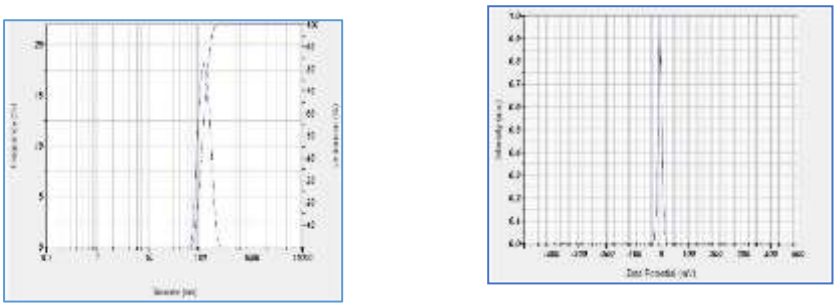
RESULTS

Physicochemical Evaluation and Optimized Batch Selection

All three formulations exhibited comparable sedimentation volumes (0.98–0.99) with no evidence of crystal growth, indicating baseline physical stability (Table 3). However**,** PHN-A demonstrated the most favorable physicochemical profile and was selected as the optimized batch. It showed excellent redispersibility, near-neutral pH (6.00) suitable for oral use, and the smallest particle size (117 nm) with the lowest polydispersity index (0.372)**,** indicating a uniform dispersion. PHN-A also exhibited the highest viscosity (93.87 cP)**,** supporting enhanced suspension stability, along with a zeta potential of −0.30 mV**.** In comparison, PHN-B and PHN-C displayed larger particle sizes,higher polydispersity, lower viscosity, and reduced redispersibility**,** reflecting comparatively lower stability. Collectively, these parameters confirm PHN-A as the most stable and homogenous formulation**,** suitable for subsequent in vivo evaluation.

Table 3: Physicochemical Characterization of Polyherbal Nanosuspension Batches (PHN-A, PHN-B, PHN-C)

Parameter	PHN-A	PHN-B	PHN-C
Sedimentation Volume (F)	0.99	0.98	0.99
Redispersibility	Excellent	Good	Poor
Flow Rate (mL/sec)	5/59	5/38	5/19
pH	6.00	5.09	5.00
Particle Size (nm)	117	126.3	210.35
Viscosity (cP)	93.87	26.09	17.24
Crystal Growth	Absent	Absent	Absent
Zeta Potential (mV)	–0.30	–0.20	–0.15
Polydispersity Index	0.372	0.486	1.221



(a) (b)

Fig1: - a) Particle size and zeta potential of optimized PHN-A**.** Particle size analysis of the optimized polyherbal nanosuspension (PHN-A) showed a single narrow distribution peak around 117 nm, indicating a uniform nanosuspension with low polydispersity. b) Zeta potential analysis showed a sharp peak near 0 mV(approximately −0.30 mV), suggesting a homogeneous particle population and stable dispersion.

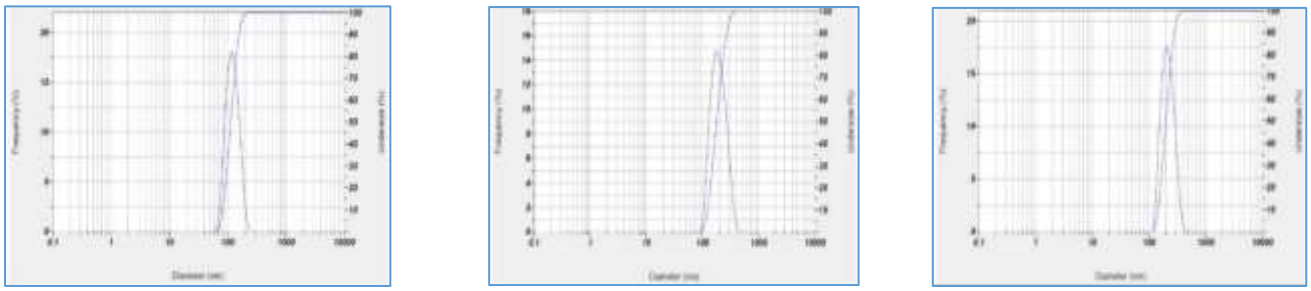
Natural Resources for Human Health
eISSN: 2583-1194

Accelerated Stability of Optimized Formulation (PHN-A)

PHN-A remained physically stable over 90 days**,** with only minor changes in key parameters. Particle size increased slightly from 117 to 128.4 nm**,** while PDI remained within an acceptable range (0.372–0.486), indicating maintained dispersion uniformity. Viscosity was largely unchanged (~93 cP), and zeta potential showed minimal fluctuation (−0.30 to −0.10 mV). Overall, the limited variation across all parameters confirms thestability and robustness of the optimized nanosuspension under accelerated conditions.

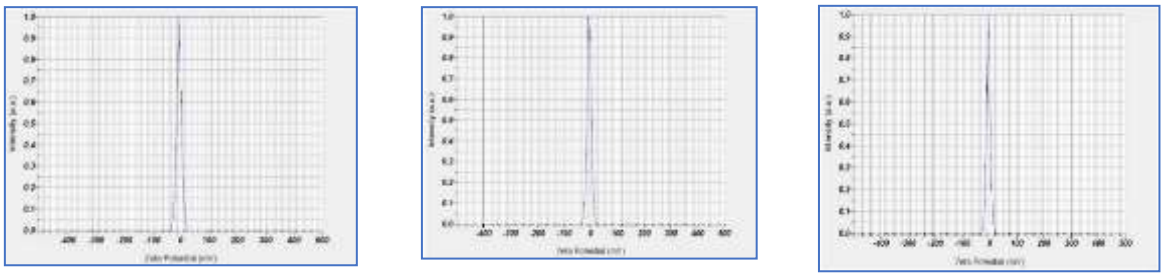
Table 4: Accelerated Stability Profile of Optimized Polyherbal Nanosuspension (PHN-A)

Time (Days)	PDI	Particle Size (nm)	Viscosity (cP)	Zeta Potential (mV)
0	0.372	117.0	93.87	–0.30
30	0.403	123.0	93.87	–0.30
60	0.486	126.3	93.00	–0.20
90	0.387	128.4	92.77	–0.10



(a) (b) (c)

Fig 2. Particle Size Distribution of Optimized Polyherbal Nanosuspension (PHN-A). Particle size profiles of PHN-A at (a) 30 days, (b) 60 days, and (c) 90 days showing a single narrow peak centered ~117–128 nm, indicating uniform particle distribution with low polydispersity. The minimal shift in peak position over time confirms stable particle size and dispersion consistency during storage. Axes: Diameter (nm) vs. frequency (%).



(a) (b) (c)

Fig 3: - Zeta Potential of Optimized Polyherbal Nanosuspension (PHN-A) Over Time. Zeta potential profiles of PHN-A at (a) 30 days, (b) 60 days, and (c) 90 days showing a single sharp peak near 0 mV (≈ −0.30 to −0.10 mV)**,** indicating stable and homogeneous dispersion over time**.**

In Vivo evaluation:-Acute Toxicity (OECD 423)

The PHN was well tolerated at an oral dose of 2000 mg/kg in rats over a 14-day observation period. No mortality, morbidity, or treatment-related adverse effects were observed. Behavioral and physiological parameters remained normal throughout,

indicating a favorable acute safety profile of the formulation. The acute oral toxicity study was performed according to OECD Guideline No. 423.

Progressive Metabolic Changes (Days 0–90)

At baseline (Day 0), all experimental groups exhibited physiological and biochemical parameters within normal reference ranges, with no significant inter-group differences ($p > 0.05$), confirming uniform starting conditions. Body weight ranged from 160.0–169.2 g, fasting blood glucose from 86.7–91.7 mg/dL, triglycerides from 66.9–89.3 mg/dL, total cholesterol from 61.7–76.7 mg/dL, HDL from 28.5–35.6 mg/dL, and LDL from 25.4–30.4 mg/dL.

After 30 days of HFD feeding, early metabolic disturbances were observed in the disease control group, with body weight reaching 206.0 ± 4.0 g, fasting glucose 99.0 ± 4.6 mg/dL, triglycerides 91.7 ± 3.4 mg/dL, and total cholesterol 89.3 ± 4.2 mg/dL. LDL increased to 40.0 ± 1.8 mg/dL compared to 30.1 ± 1.6 mg/dL in the normal control, indicating early atherogenic changes. Treatment groups showed partial regulation, with lower triglyceride levels(e.g., 67.6 ± 3.5 mg/dL in the low-dose group), although full metabolic syndrome was not yet established.

By Day 60, pronounced metabolic alterations were evident in the HFD group. Body weight increased to 280.00 ± 4.27 g compared to 219.17 ± 3.46 g in normal control. Fasting glucose rose to 111.33 ± 4.27 mg/dL, triglycerides to 133.45 ± 1.25 mg/dL, and total cholesterol to 120.31 ± 2.55 mg/dL. LDL showed a marked increase to 61.82 ± 1.21 mg/dL, while HDL declined to 29.22 ± 1.17 mg/dL, indicating advancing dyslipidemia and impaired metabolic regulation.

At Day 90, the HFD disease control group exhibited the full constellation of metabolic syndrome. Body weight reached 330.00 ± 4.02 g versus 232.83 ± 3.02 g in normal control. Fasting blood glucose increased to 136.83 ± 4.19 mg/dL, triglycerides to 223.35 ± 1.43 mg/dL, and total cholesterol to 150.16 ± 2.39 mg/dL. LDL rose markedlyto 90.34 ± 1.54 mg/dL, while HDL declined to 25.04 ± 1.15 mg/dL. Hepatic enzymes were also elevated, with SGPT (ALT) at 89.25 ± 2.05 IU/L and SGOT (AST) at 154.37 ± 1.69 IU/L, indicating significant hepatic stress and lipid accumulation.

At Day 120, the HFD disease control group showed persistent and progressive metabolic abnormalities, confirming the chronic nature of diet-induced metabolic syndrome. Body weight increased to 404.0 g (vs. 268.3 g in normal control). Fasting blood glucose remained markedly elevated at 139.0 mg/dL, indicating severe insulin resistance. Dyslipidemia persisted, with elevated triglycerides and total cholesterol, along with abnormal HDL and LDL levels. Hepatic injury markers were also increased, with SGPT (ALT) at 120.31IU/L and SGOT(AST) 153.35, indicating progressive hepatic steatosis and inflammation. In contrast, PHN treatment demonstrated dose-dependent therapeutic improvement. At 200 mg/kg, body weight was 362.0 g, while at 400 mg/kg it decreased to 326.8 g (vs. 404.0 g in HFD control). Fasting glucose improved from 139.0 mg/dL to 110.0 mg/dL (LD to HD). Triglycerides decreased from 109.10 mg/dL (LD)to 93.15 mg/dL (HD), and total cholesterol from 116.60 to 86.16 mg/dL. Hepatic markers showed marked improvement, with SGPT (ALT) reduced to 45.41 IU/L (HD)and SGOT(AST) 91.00 IU/L (HD)

Notably, the high-dose group (400 mg/kg) demonstrated effects comparable to or exceeding the standard drug (Orlistat) across most parameters, confirming clinically relevant, dose-dependent efficacy of the polyherbal formulation.

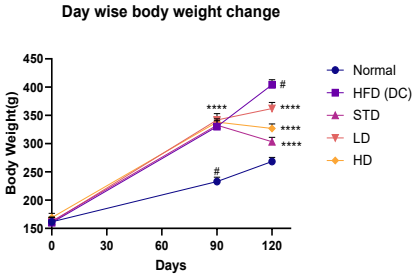
Treatment with the test compound significantly improved adipocyte morphology in HFD-induced animals. The high-dose group (400 mg/kg) showed the most effective reduction in adipocyte diameter, area, and adipocyte index, from 80.17 ± 3.54 to 31.83 ± 1.33 (HD) indicating strong protection against adipocyte hypertrophy and obesity-related adipose tissue changes.

Anti-oxidant Activity

SOD levels were notably higher in the HFD group in comparison to Normal, STD, LD, and HD, indicating increased oxidative stress in the diseased condition. LD levels remained near the disease control (ns), indicating no significant antioxidant effect at that dosage, while both STD and HD significantly reduced SOD, with HD showing results similar to STD. The HFD group demonstrated a significant increase in GSH compared to Normal, STD, LD, and HD, aligning with a compensatory antioxidant reaction to ongoing oxidative stress. Similar to SOD, LD did not show a separation from the disease control (ns), whereas STD and HD successfully lowered GSH back to normal levels. Catalase activity was significantly greater in the HFD group compared to the Normal, STD, LD, and HD groups. LD once more showed no notable decrease in comparison to DC (ns). Both STD and HD markedly reduced CAT activity, while LD consistently emerged as the least effective dosage among the three oxidative

stress markers. The 400 mg/kg dose demonstrated superior therapeutic effectiveness alongside dose-dependent metabolic and hepatoprotective effects.

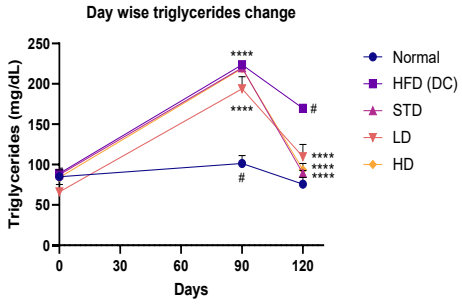
Fig 4:- Effect of PHN on body weight (a), glucose (b) Insulin (c) triglyceride (d) cholesterol (e) HDL (f) LDL (g) SGPT (h) SGOT



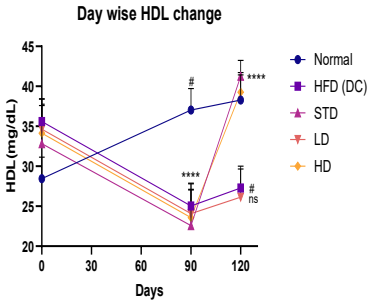
(a)



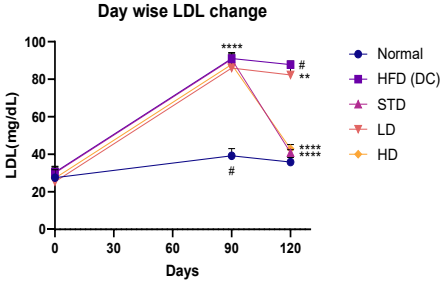
(b)



(c)

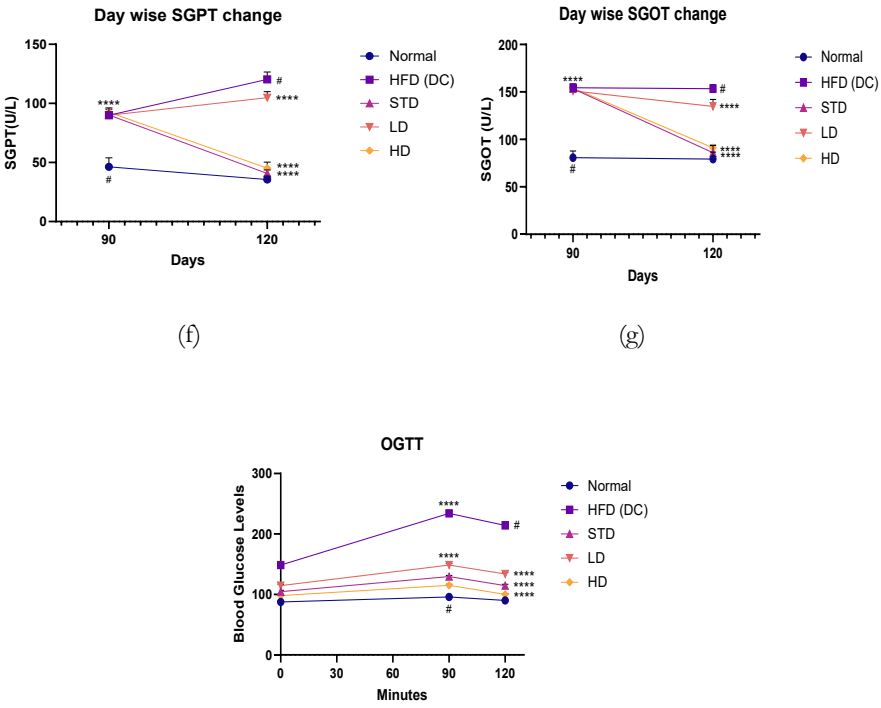


(d)



(e)

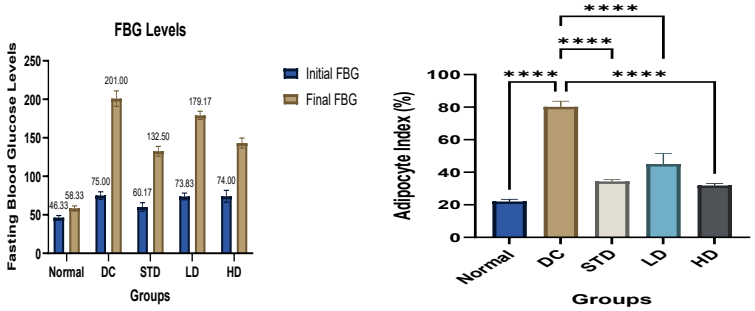
Natural Resources for Human Health
eISSN: 2583-1194



(f) (g)

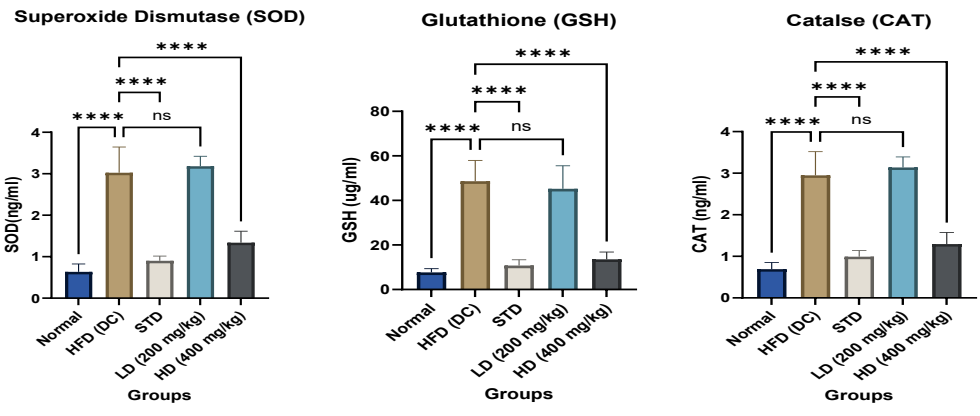
(h)

Fig 5: Effect of Treatment on a) Fasting Blood Glucose Levels b) Adipocyte Index Parameters



(a) **(b)**

Fig 6: Effect of Treatment on Antioxidant Parameters a) SOD b) GSH c) CAT



(a) **(b)** **(c)**

DISCUSSION

Because of its complex pathophysiology, which includes oxidative stress, dyslipidemia, insulin resistance, and hepatic steatosis, metabolic syndrome is challenging to treat. Conventional single-target medicines might have negative side effects and sometimes provide only partial benefits. In light of this, the optimized polyherbal nanosuspension PHN-A resulted in multi-target benefits in a rat model caused by a high-fat diet that mimics key aspects of the human metabolic syndrome. The formulation's tiny particle size (117 nm), appropriate viscosity, low polydispersity, and 90-day storage stability are all in line with the phytochemicals' improved oral bioavailability and solubility. Its favorable acute toxicity profile—no clinical symptoms or fatality at 2000 mg/kg—further demonstrates that it is suitable for oral administration. PHN-A clearly reversed dose-dependent increases in body weight, fasting glucose, triglycerides, total cholesterol, LDL, hepatic transaminases, and decreased HDL in the HFD model. The high dosage (400 mg/kg) decreased the adipocyte index, suggesting attenuation of adipose-tissue hypertrophy, and matched or surpassed the effects of orlistat (45 mg/kg). Rather than merely compensatory overexpression, concurrent normalization of the increased antioxidant markers SOD, GSH, and CAT suggests successful redox imbalance correction. The HFD treatment mainly caused metabolic and hepatic changes over the research period, as evidenced by the cardiac morphology remaining essentially normal. When combined, PHN-A concurrently targets many key metabolic syndrome pathophysiological sites. Strengthening translational potential will need pharmacokinetic characterization, longer-term safety assessment, and mechanistic investigations in other animals. All things considered, the results validate PHN-A as a viable multi-target nanoformulation approach for metabolic syndrome.

CONCLUSION

Equal amounts of alcoholic extracts of *Tinospora cordifolia, Momordica charantia, Trigonella foenum-graecum, Acorus calamus, and Tecomella undulata* were used to create an optimized polyherbal nanosuspension (PHN-A). The formulation demonstrated an outstanding acute safety profile, acceptable physicochemical qualities, and physical stability for ninety days. PHN-A, especially at 400 mg/kg, clearly and dose-dependently improved body weight, lipid profile, glycemic control, and hepatic enzyme levels in a rat model of metabolic syndrome caused by a high-fat diet. important metabolic enzymes and antioxidant levels. Alongside these biochemical advantages, the architecture of the liver and pancreas was histologically restored. PHN-A's promise as a promising candidate formulation for the treatment of metabolic syndrome is supported by its collective multi-target effects. To validate long-term effectiveness, safety, and mechanism of action, more preclinical and clinical research is required.

Conflict of interest

The authors declare no conflict of interest.

Funding

The research was self-funded.

Declaration of Competing Interest

The authors declare that they have no known competing financial interests or personal relationships that could have

appeared to influence the work reported in this paper.

Acknowledgments

Authors thank the management of Tatyasheb Kore College of

Pharmacy Warananagar, The authors also thank the Dr. Sandip Patil, Dr, Ajit Patil, Mr. Aditya, Mr. Pranav

to carry out the research process with all the help required.

REFERENCES

[1] Noeman SA, Hamooda HE, Baalash AA. Biochemical study of oxidative stress markers in the liver, kidney and heart of high fat diet induced obesity in rats. Diabetology & metabolic syndrome. 2011 Aug 3;3(1):17.

[2] Ansari P, Flatt PR, Harriott P, Abdel-Wahab YH. Evaluation of the antidiabetic and insulin releasing effects of A. Squamosa, including isolation and characterization of active phytochemicals. Plants. 2020 Oct 12;9(10):1348.

[3] Sharma P, Singh S, Sharma N, Singla D, Guarve K, Grewal AS. Targeting human Glucokinase for the treatment of type 2 diabetes: an overview of allosteric Glucokinase activators. Journal of Diabetes & Metabolic Disorders. 2022 Jun;21(1):1129-37.
[4] Matschinsky FM. Assessing the potential of glucokinase activators in diabetes therapy. Nature reviews Drug discovery. 2009 May;8(5):399-416.
[5] Haddad D, Dsouza VS, Al-Mulla F, Al Madhoun A. New-generation glucokinase activators: potential game-changers in type 2 diabetes treatment. International Journal of Molecular Sciences. 2024 Jan 1;25(1):571.
[6] Ashcroft FM, Lloyd M, Haythorne EA. Glucokinase activity in diabetes: too much of a good thing?. Trends in Endocrinology & Metabolism. 2023 Feb 1;34(2):119-30.
[7] Nakamura A, Terauchi Y, Ohyama S, Kubota J, Shimazaki H, Nambu T, Takamoto I, Kubota N, Eiki J, Yoshioka N, Kadowaki T. Impact of small-molecule glucokinase activator on glucose metabolism and β-cell mass. Endocrinology. 2009 Mar 1;150(3):1147-54.
[8] Chiba K, Nomoto H, Izumihara R, Zhang X, Kameda H, Nakamura A, Atsumi T. Metabolic adaptation to acute metabolic stress via PFKFB3 upregulation in rodent beta cells. Frontiers in Endocrinology. 2025 Jun 17;16:1552700.
[9] Togashi Y, Shirakawa J, Orime K, Kaji M, Sakamoto E, Tajima K, Inoue H, Nakamura A, Tochino Y, Goshima Y, Shimomura I. B-Cell proliferation after a partial pancreatectomy is independent of IRS-2 in mice. Endocrinology. 2014 May 1;155(5):1643-52.
[10] Rajas F, Gautier-Stein A, Mithieux G. Glucose-6 phosphate, a central hub for liver carbohydrate metabolism. Metabolites. 2019 Nov 20;9(12):282.
[11] Song J, Sun H, Zhang S, Shan C. The multiple roles of glucose-6-phosphate dehydrogenase in tumorigenesis and cancer chemoresistance. Life. 2022 Feb 12;12(2):271.
[12] Kwaifa IK, Erhabor O, Yakubu A, Bagudo AI, Ali BH, Uchechukwu OF, Bunza NM, Kalgo MU, Isiyaku A, Yeldu M, Isah D. Pathophysiology and Current Laboratory Investigations of Glucose-6-Phosphate Dehydrogenase Deficiency. Sokoto Journal of Medical Laboratory Science. 2025 May 30;10(1).
[13] Ravikumar N, Greenfield G. Glucose-6-phosphate dehydrogenase deficiency: a review. International Journal of Medical Students. 2020 Dec 17;8(3):281-7.
[14] Pes GM, Dore MP. Acquired glucose-6-phosphate dehydrogenase deficiency. Journal of Clinical Medicine. 2022 Nov 11;11(22):6689.
[15] Sarsenbayeva A, Jui BN, Fanni G, Barbosa P, Ahmed F, Kristófi R, Cen J, Chowdhury A, Skrtic S, Bergsten P, Fall T. Impaired HMG-coa reductase activity caused by genetic variants or statin exposure: impact on human adipose tissue, β-cells and metabolome. Metabolites. 2021 Aug 25;11(9):574.
[16] González-Lleó AM, Sánchez-Hernández RM, Boronat M, Wägner AM. Diabetes and familial hypercholesterolemia: interplay between lipid and glucose metabolism. Nutrients. 2022 Apr 3;14(7):1503.
[17] Xiao X, Luo Y, Peng D. Updated understanding of the crosstalk between glucose/insulin and cholesterol metabolism. Frontiers in Cardiovascular Medicine. 2022 Apr 29;9:879355.
[18] Van Stee MF, de Graaf AA, Groen AK. Actions of metformin and statins on lipid and glucose metabolism and possible benefit of combination therapy. Cardiovascular diabetology. 2018 Jun 30;17(1):94.
[19] Ashrafizadeh H, Oroojan AA, Ahmadi I, An'aam M. The Role of Statins (HMG-coa Reductase Inhibitors) on Insulin Secretion from the Islets of Langerhans: A Systematic Review. Jentashapir Journal of Cellular and Molecular Biology. 2022;13(2).
[20] Wang HJ, Park JY, Choe EY, Kwon O, Lee YH, Kim G, Bae J, Park SH, Yun YJ, Yun M, Kim CH. Chronic HMG-coa Reductase Inhibitor Treatment Contributes to Dysglycemia by Up-Regulating Hepatic Gluconeogenesis through Autophagy Induction. Indiabetes 2014 Jun 1 (Vol. 63, pp. A461-A461). 1701 N BEAUREGARD ST, ALEXANDRIA, VA 22311-1717 USA: AMER DIABETES ASSOC.
[21] Kim K, Chini N, Fairchild DG, Engle SK, Reagan WJ, Summers SD, Mirsalis JC. Evaluation of cardiac toxicity biomarkers in rats from different laboratories. Toxicologic pathology. 2016 Dec;44(8):1072-83.
[22] Bhatti MI, Memon AR, Laghari MJ, Memon RA, Laghari S, Memon FR, Shams S. Role of glucose 6 phosphate dehydrogenase (G6PD) in diabetic cataract. J. Pharm. Res. Int. 2021 Dec 23;33(60):1646-51.
[23] Farhangi MA, Mesgari-Abbasi M, Hajiluian G, Nameni G, Shahabi P. Adipose tissue inflammation and oxidative stress: the ameliorative effects of vitamin D. Inflammation. 2017 Oct;40(5):1688-97.

[24] Farhangi MA, Nameni G, Hajiluian G, Mesgari-Abbasi M. Cardiac tissue oxidative stress and inflammation after vitamin D administrations in high fat-diet induced obese rats. BMC cardiovascular disorders. 2017 Jun 19;17(1):161.